

FDTD Simulation of Exposure of Biological Material to Electromagnetic Nanopulses

Neven Simicevic^{†§} and Donald T. Haynie[‡]

[†] Center for Applied Physics Studies, Louisiana Tech University, Ruston, LA 71272, USA

[‡] Center for Applied Physics Studies, Biomedical Engineering and Institute for Micromanufacturing, Louisiana Tech University, Ruston, LA 71272, USA

Abstract.

Ultra-wideband (UWB) electromagnetic pulses of nanosecond duration, or nanopulses, are of considerable interest to the communications industry and are being explored for various applications in biotechnology and medicine. The propagation of a nanopulse through biological matter has been computed in the time domain using the finite difference-time domain method (FDTD). The approach required existing Cole-Cole model-based descriptions of dielectric properties of biological matter to be re-parametrized using the Debye model, but without loss of accuracy. The approach has been applied to several tissue types. Results show that the electromagnetic field inside a biological tissue depends on incident pulse rise time and width. Rise time dominates pulse behavior inside a tissue as conductivity increases. It has also been found that the amount of energy deposited by 20 kV/m nanopulses is insufficient to change the temperature of the exposed material for the pulse repetition rates of 1 MHz or less.

PACS numbers: 87.50.Rr, 87.17.d, 77.22.Ch, 02.60.x

1. Introduction

A facility for bioelectromagnetics research has recently been established at Louisiana Tech University (LA Tech) through sponsorship by Air Force Office of Scientific Research. LA Tech leads a multi-university collaboration in this area which involves three other institutions in north Louisiana: Grambling State University, University of Louisiana at Monroe, and Louisiana State University-Health Sciences Center, Shreveport. Current focus of research is bioeffects of non-ionizing ultra-wideband (UWB) electromagnetic (EM) pulses of nanosecond duration, or nanopulses. The research program encompasses experimental studies of biological matter, equipment design and fabrication, and computational modeling. Goals of the research include providing a sound basis for nanopulse exposure safety standards.

The literature on UWB radiation is extensive [1]. In the present work, a nanopulse is a rapid, transient change in amplitude, from a baseline to peak, followed by a relatively rapid return to baseline. It is a short duration, high-intensity burst of electromagnetic energy. In the LA Tech bioelectromagnetics facility, fondly known as the Nanopulse Factory, a typical nanopulse has a width of 1-10 *ns*, a rise time of ~ 100 *ps*, and an amplitude of ~ 20 *kV/m*.

Extensive research has been done on biological effects of EM fields. Detailed descriptions are provided in Reference [2]. Bioeffects of nanopulses, however, may be qualitatively different from those of narrow-band radiofrequencies. The LA Tech-led collaboration is currently testing nanopulse bioeffects using a range of model systems. At the cellular level this includes *E. coli*, photosynthetic bacteria, bovine red blood cells, bovine platelets, mouse hepatocytes, mouse mammary epithelial cells, and human dermal fibroblasts; that is, both prokaryotes and eukaryotes. The main sub-cellular model is horseradish peroxidase. A whole animal model is *C. elegans*.

The basic exposure equipment consists of a pulse generator, a parallel-plate transmission line (*e.g.* gigahertz transverse electromagnetic mode or GTEM cell), measuring/recording instruments, and a radiofrequency enclosure (screen room, Faraday cage). A schematic is shown in Figure 1. Output of a commercial or home-built nanosecond pulse generator [3] is fed into the GTEM cell or a home-built parallel-plate capacitor, through which the pulse propagates virtually unperturbed to the position of the sample.

Pulse generator output is measured and recorded using a digital storage oscilloscope. Nevertheless, it is a challenge to make accurate real-time measurements of the electric field in an exposure chamber in the vicinity of the sample, and it is practically impossible to measure the field inside the sample in real time. To find the field inside a sample, which is what one cares about, it is necessary to consider a computational approach.

The interaction of short EM pulses and biological matter has not been modeled in such detail as the interaction of radio frequency radiation. A number of computational approaches exist for modeling the experimental apparatus, biological cell, and cellular environment, and the EM interaction mechanisms and their effects [2]. The complexity

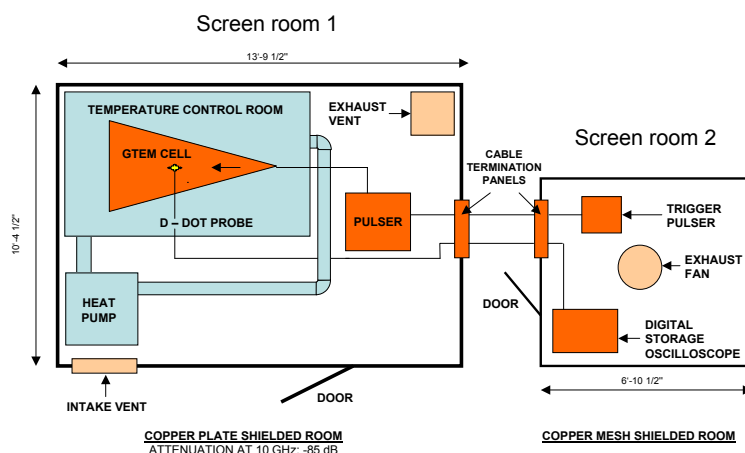


Figure 1. Schematic of LA Tech nanopulse exposure facility. It consists of two Faraday cages, the GTEM cell and pulser in one and the measuring/recording instruments in the other.

of any realistic situation requires a numerical rather than an analytical approach. The latter, however, should be taken in parallel with the former, since the dynamic range of the problem could span many orders of magnitude in some physical quantities and an “external” check on computational method is needed. In the case of a biological cell, for example, the length scale ranges over nine orders of magnitude, from the thickness of the plasma membrane to the size of the exposure chamber. This represents a considerable challenge for any numerical method.

For the calculations described in the present work, finite-difference time domain FDTD was applied. This method of solving Maxwell’s equations is relatively simple, can easily deal with a broadband response, has almost no limit in the description of geometrical and dispersive properties of the material being simulated, is numerically robust, and is appropriate for the computer technology of today. Originally introduced by Kane Yee in the 1960s [4], FDTD was developed extensively in the 1990s [5, 6, 7, 8], owing in part to the increasing availability of fast computers. In this paper we describe FDTD calculations of the EM field inside samples exposed to nanopulses in a GTEM cell. The EM properties of the environment are included in the calculation to the fullest extent. The object is to advance understanding of dominant mechanisms of interaction of nanopulses with biological structures.

2. Computational Inputs

In order to characterize the response of a biological system to an EM pulse, two important quantities must be known with a reasonable degree of precision: the value of the field surrounding the system and in the system, and the extent of conversion of EM energy into mechanical or thermal energy, both in the system itself and in the surroundings. FDTD has been applied for this purpose, and an original set of

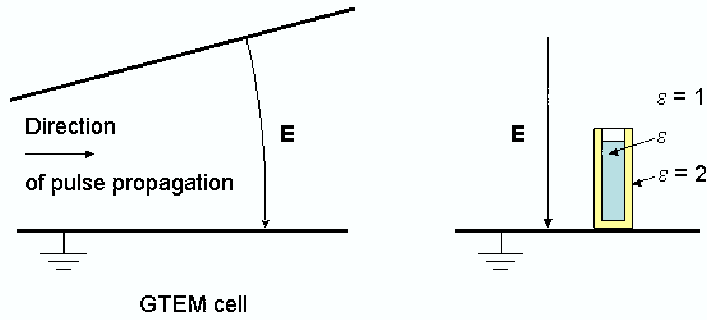


Figure 2. Geometry of exposed sample: cuvette inside the GTEM cell.

computer programs has been developed at LA Tech to compute the EM field in any dimension for almost any choice of geometry and EM properties of a material. Some of the computations were performed using a 3-dimensional model, the results presented here, however, were obtained using 2-dimensional FDTD. The approach was based on the following dimensions: samples in a cuvette ($1\text{ cm} \times 1\text{ cm} \times 4.5\text{ cm}$, with 1mm thick walls), and a GTEM cell in which exposure occurs ($8\text{ cm} \times 8\text{ cm}$ at inlet, $58\text{ cm} \times 58\text{ cm}$ at absorbing cones, and 100 cm long). 2-dimensional FDTD reduces the computation time without compromising essential features of the solution. Geometry of the exposed sample is shown in Figure 2.

Each calculation depends on the shape of nanopulses fed into the GTEM cell, defined geometrical properties of the exposed “system”, and its dispersive or dielectric properties (including conductivity). It was important that each property be both realistic and appropriate for numerical simulation. Further details of each feature are given in the following subsections.

2.1. Electromagnetic Pulse Inside GTEM Cell

The EM field of a nanopulse inside a GTEM cell can be measured when the cell is empty [9]. FDTD calculation of pulse propagation through a flared transmission line shows that the shape of the pulse is preserved as it propagates and, as expected, only the amplitude decreases. This agrees with the results of work done at Brooks Air Force Base (now Brooks City-Base) on modeling a GTEM cell [10]. The pulse in a GTEM cell can be described as a double exponential function:

$$E = E_0(e^{-\alpha t} - e^{-\beta t}), \quad (1)$$

where E_0 is pulse amplitude and α and β coefficients describing pulse rise time, fall time, and width. Parameters that describe pulse shape in the empty GTEM cell at LA Tech in the vicinity of the region under test (sample position) are $E_0 = 18.5\text{ kV/m}$, $\alpha = 1. \times 10^8\text{ s}^{-1}$, and $\beta = 2. \times 10^{10}\text{ s}^{-1}$. This pulse, having a rise time of 150 ps and width of 10 ns , was the input in the present work.

2.2. Geometrical Properties of Exposed Sample

Most biological specimens in experiments in the LA Tech-led research program consist of mammalian cells or microorganisms (length ≤ 1 mm). This size is small in comparison to the dimensions of the GTEM cell and will not perturb the general character of the EM field. In other words, the character of the field, anywhere in a GTEM cell except in the vicinity of the sample, will be roughly the same as in an empty cell. The largest object in the GTEM cell during an experiment is the sample container. Ordinarily this will be a polystyrene cuvette, whose shape and dimensions are shown in Figure 3, a Petri dish, or a 96-, 48-, or 8-well plate.

Other considerations must be made when describing geometrical properties of an object in an FDTD simulation. The method requires space and time to be discretized. The discretization of space is done by means of Yee cells, cuboids having edge lengths Δx , Δy , and Δz . If $\Delta x = \Delta y = \Delta z$, a Yee cell represents a discrete cube of space. The discretization of time is obtained from the size of the Yee cell by imposing the Courant stability criterion:

$$\Delta t \leq \frac{1}{c\sqrt{(\Delta x)^2 + (\Delta y)^2 + (\Delta z)^2}}, \quad (2)$$

where c is the speed of light.

Yee cell must be small enough not to distort the shape of the sample container, has to account for the full frequency range of the EM pulse, and must be large enough for the time step to be practical for overall computation. Its size is related to the highest frequency which needs to be considered, f_{max} , by an accepted rule

$$\Delta x \simeq \frac{c}{10 f_{max}}, \quad (3)$$

where c is the speed of light and f_{max} is a cut-off frequency above which the calculation becomes unreliable for the chosen cell size. In the present work the maximum considered frequency was $f_{max} = 100$ GHz, which required the size of the Yee cube edge lengths to be $\Delta x = \Delta y = \Delta z \simeq 0.3$ mm. A cell edge length of $1/4$ mm satisfies the frequency criterion and is small enough to describe the shape of the sample, and derived time step satisfying the Courant stability criterion, $\Delta t \simeq 0.6$ ps, is large enough to allow the entire calculation to be performed in about 50,000 steps.

It is not always possible to achieve optimal agreement between geometrical and physical descriptions of a situation. Fortuitous circumstances in the present work minimized the number of computational operations, eliminated need of additional approximations, and allowed the entire 2-dimensional FDTD calculation to be performed on a modern computer in about 10 minutes.

2.3. Dielectric Properties of Exposed Sample

Dielectric properties of the exposed sample were treated using a recursive convolution scheme [12]. Briefly, a relation between the electric flux density, \vec{D} , and the electric

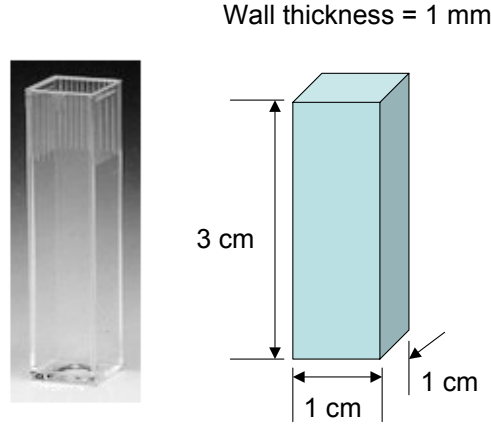


Figure 3. Shape and dimension of a cuvette used in experiment and studies described here.

field strength, \vec{E} , at points in the material at which the field was calculated, for a monochromatic EM wave, is

$$\vec{D}(\omega) = \epsilon(\omega)\vec{E}(\omega). \quad (4)$$

Electric permittivity $\epsilon(\omega)$ is a function of frequency ω of the monochromatic wave. FDTD requires a connection between \vec{D} and \vec{E} in the time domain, which can be found by Fourier transformation of Equation 4. The result can be written as [11]

$$\vec{D}(t) = \epsilon_0\vec{E}(t) + \epsilon_0 \int_0^t \chi(\tau)\vec{E}(t - \tau) d\tau. \quad (5)$$

where ϵ_0 is the permittivity of free space, and $\chi(\tau)$, the electric susceptibility of a material, is described by the following Fourier transform:

$$\chi(\tau) = \frac{1}{2\pi} \int_{-\infty}^{+\infty} (\epsilon(\omega)/\epsilon_0 + 1)e^{-i\omega\tau} d\omega. \quad (6)$$

In FDTD all physical quantities are discretized and

$$\vec{D}(t) \mapsto \vec{D}(n\Delta t) = \epsilon_\infty\epsilon_0\vec{E}(n\Delta t) + \epsilon_0 \int_0^{n\Delta t} \chi(\tau)\vec{E}(n\Delta t - \tau) d\tau. \quad (7)$$

The quantity ϵ_∞ describes the property of the material at frequencies approaching infinity, and n is a time step of length Δt . Without going into details of FDTD, which in any case can be found in References [12, 13, 15], the value of each vector component in Equation 7 at time step n can be written in discrete form as

$$D^n = \epsilon_\infty\epsilon_0 E^n + \epsilon_0 \sum_{m=0}^{n-1} E^{n-m} \chi_m, \quad (8)$$

where

$$\chi_m = \int_{m\Delta t}^{(m+1)\Delta t} \chi(\tau) d\tau. \quad (9)$$

EM properties of a biological material are normally expressed in terms of frequency-dependent dielectric properties and conductivity. They have been measured and modeled for over a 100 years, and a great deal of information on them is available in the literature [2]. Data used in the present work are from References [16] and [17], where the measured values of 45 tissues were parametrized using the Cole-Cole model:

$$\epsilon(\omega) = \epsilon_{\infty} + \sum_{k=1}^4 \frac{\Delta\epsilon_k}{1 + (i\omega\tau_k)^{1-\alpha}} + \frac{\sigma}{i\omega\epsilon_0}, \quad (10)$$

where $i = \sqrt{-1}$. Permittivity in the terahertz frequency range ϵ_{∞} , drop in permittivity in a specified frequency range $\Delta\epsilon_k$, coefficient α , relaxation time τ , and the ionic conductivity σ , constitute up to 14 real parameters of the fit. This approach can generally be used with confidence for frequencies above 1 *MHz* [16], the frequency range of interest in nanopulse bioeffects study. A plot of all the fit curves [16] reveals similarities of the dispersive properties of the various tissues.

While formally the electric susceptibility is just a Fourier transformation of Equation 10, the transformation is hardly easy [18] and can only be achieved numerically. An example of a numerical Fourier transformation of a Cole-Cole expression, Equation 10, for blood is shown in Figure 4. Although this simple function can be modeled with just one free parameter, its application is problematic.

Cole-Cole parametrization can provide a useful empirical description of the dielectric properties of tissues over a broad frequency range. This model, however, does not reflect a specific underlying physical mechanism, as it is apparent from the divergence of $\epsilon(\omega)$ as the frequency goes to infinity when it should go to unity [19]. In addition, the components of the electric displacement \vec{D} , are calculated as a convolution of the electric field and material susceptibility, Equation 5. The response of a material to an external EM pulse is very fast. Susceptibility, as shown in Figure 4, is largest at the beginning of the response. Hence, precisely in the most important region for evaluating the integral in Equation 5 information on susceptibility will not exist. The time step in calculating \vec{D} using Equation 8 was 0.6 *ps*. The first several steps of the computation therefore required the use of an extrapolated value of susceptibility. Because the Cole-Cole expression does not describe a physical mechanism, making such extrapolation has dubious validity and could represent a substantial source of error.

There is another difficulty in applying the Cole-Cole parametrization. Numerically, the electric displacement is calculated by Equation 8 as part of the overall Yee algorithm [4, 13, 14, 15]. Evaluation of the integral in Equation 9 for all Yee cells at each time step, however, will be extremely time consuming for even the most effective integration techniques.

Both problems - extrapolation of susceptibility and numerical evaluation of Equation 9 - are more satisfactorily solved if Debye parametrization is substituted for Cole-Cole parametrization. The Debye model describes relaxation of a material at the molecular level using an exponential function defined by a relaxation time τ . In place

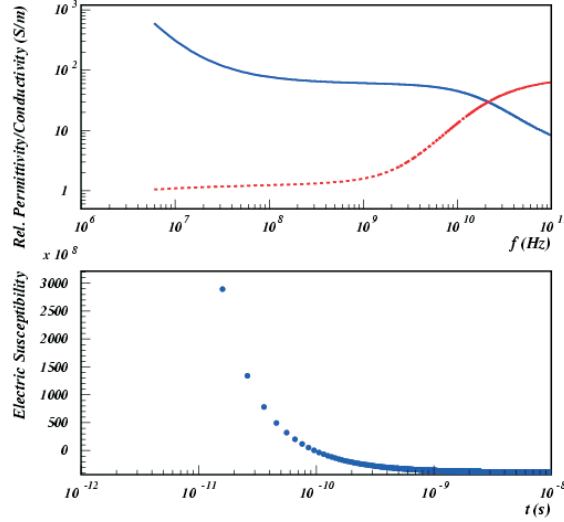


Figure 4. Top, relative permittivity (solid line) and conductivity (dashed line) of blood in the frequency range ≤ 100 GHz, calculated by Equation 10 as parametrized in References [16] and [17]. Bottom, the electric susceptibility obtained by numerical Fourier transformation of the same equation.

of Equation 10, neglecting conductivity σ for the moment, dielectric properties of a material can be described as

$$\epsilon(\omega) = \epsilon_{\infty} + \sum_{k=1}^N \frac{\Delta\epsilon_k}{1 + i\omega\tau_k} = \epsilon_{\infty} + \sum_{k=1}^N \chi_k(\omega), \quad (11)$$

where N is the number of independent first-order processes. Response of the dielectric material to an external field in the time domain can be obtained by Fourier transformation of each independent first-order process $\chi_k(\omega)$ in Equation 11:

$$\chi_k(t) = \frac{\Delta\epsilon_k}{\tau_k} e^{-t/\tau_k}, \quad t \geq 0. \quad (12)$$

where τ_k is the relaxation time for process k .

As to static conductivity σ , it is defined in the time domain as the constant of proportionality between the current density \vec{J} and the applied electric field \vec{E} as $\vec{J} = \sigma\vec{E}$. It is important to mention that its implementation in FDTD does not require additional or different Fourier transforms [6]. The dependence of \vec{J} on \vec{E} in the conductive material is simply

$$\vec{J} = \sigma\vec{E} + \sum_{k=1}^N \frac{\Delta\epsilon_k\epsilon_0}{\tau_k} e^{-t/\tau_k} \vec{E}, \quad t \geq 0. \quad (13)$$

The second term represents the effects of dielectric properties of the material.

The advantage of Debye parametrization becomes clear when evaluating Equations 8 and 9. After including the permittivity from Equation 8 in Equation 9, it follows, for each independent first-order process, that

$$\chi_{m+1} = \frac{\Delta\epsilon}{\tau} \int_{(m+1)\Delta t}^{(m+2)\Delta t} e^{-t/\tau} dt = \Delta\epsilon e^{-(m+1)\Delta t/\tau} (1 - e^{-\Delta t/\tau}) = e^{-\Delta t/\tau} \chi_m. \quad (14)$$

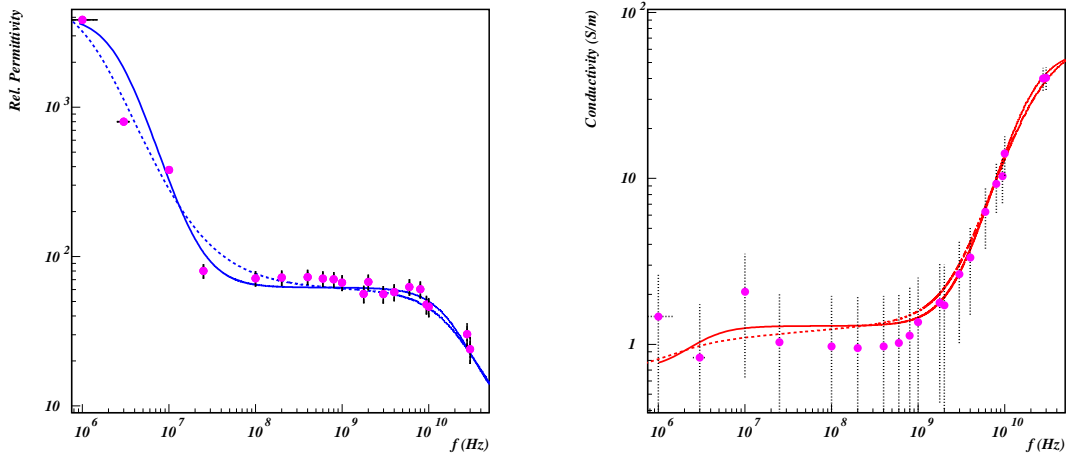


Figure 5. Relative permittivity (left) and conductivity (right) of blood parametrized by the Debye model (Equation 11; solid line) and the Cole-Cole model (Equation 10; dashed line). Data are from References [20, 21, 22, 23, 24, 25, 26].

From this it follows that the permittivity at time step $(m + 1)$ is simply the permittivity at time step m multiplied by a constant. A detailed description of this approach is given in Reference [6].

The Debye parametrization thus solves all the indicated problems associated with Cole-Cole parametrization. It remains to be determined, however, whether the Debye approach also provides a sufficiently accurate description of physical properties of a biological material. To ascertain this, we compared the Debye and Cole-Cole models in the case of blood. As shown in Figure 5, the two parameterizations describe equally well data from References [20, 21, 22, 23, 24, 25, 26] in the frequency range 1 MHz - 100 GHz , important for nanopulse research. It can be concluded that replacing the Cole-Cole model with the Debye model does not compromise the level of description of physical properties of the material.

3. Field Calculation

Above we outlined an approach to applying FDTD to calculate an EM field based on the Debye model and compared it to the Cole-Cole model. Requirements include a description of the source field and of the geometry and electromagnetic properties of the material that is both accurate and suitable for computational modeling. Now we present some results of calculations more specifically pertinent to nanopulse bioeffects research.

The cuvette shown in Figure 3 was exposed to the EM pulse described by Equation 1. Electrical properties of the material inside the cuvette were described

Material	ϵ_∞	ϵ_{s1}	ϵ_{s2}	$\tau_1(s)$	$\tau_2(s)$	$\sigma(S/m)$
Plastic	2.0	-	-	-	-	0.
Water	4.9	80.1	-	$10.0 \cdot 10^{-12}$	-	0.
Ionized Water	4.9	80.1	-	$10.0 \cdot 10^{-12}$	-	Variable
Blood	7.0	4007.0	62.0	$6.0 \cdot 10^{-8}$	$8.37 \cdot 10^{-12}$	0.7
Bone (Cancellous)	2.5	97.5	11.0	$1.5 \cdot 10^{-8}$	$8.37 \cdot 10^{-12}$	0.07
Bone (Cortical)	2.5	37.5	5.5	$1.5 \cdot 10^{-8}$	$8.37 \cdot 10^{-12}$	0.02

Table 1. Debye parameters for the materials used in the computation. Parameters for water are based on Reference [27]. Parameters for blood and bones are from a fit to data in Reference [16]. Static conductivity, σ , is also from Reference [16].

by Equation 11, explicitly written as

$$\epsilon(\omega) = \epsilon_\infty + \frac{\epsilon_{s1} - \epsilon_\infty}{1 + i\omega\tau_1} + \frac{\epsilon_{s2} - \epsilon_\infty}{1 + i\omega\tau_2}. \quad (15)$$

Parameters of materials used in the calculations are presented in Table 1. The choice of materials was intended to provide a close approximation of the materials in the experimental work of the LA Tech-led collaboration.

FDTD calculations of exposure of a biomaterial to a nanopulse provide a description of the field throughout the time range. This enables the creation of animated movies and analysis of the behavior of the EM field in time. Snapshots only can be presented here. As an example, Figure 6 shows penetration of an EM pulse in a cuvette filled with blood. The complete animation can be accessed on-line [28].

Properties of exposing the blood-filled cuvette to a linearly-polarized EM pulse described by Equation 1 can be summarized as follows:

- Penetration of the electric component is defined substantially more by pulse rise time than pulse width, and the width inside the blood sample is an order of magnitude shorter than the width of the incident pulse (Figure 7). The component of the electric field in the direction of polarization (y) is at least a factor of two larger than the component induced in the perpendicular direction (x).
- The magnetic field component in the material is dominated at first by rise-time induction and then, as the penetrated electric field components fall to zero, behaves as though no material were present (Figure 8).

Ionized water of the conductivity of blood gave essentially the same result as blood. This means that in nanopulse research the dielectric properties of biological matter are dominated by those of water at high frequencies. It follows that model parameterization at high frequencies is important for describing the propagation of a nanopulse in biological matter.

For pure water the situation can be summarized as follows:

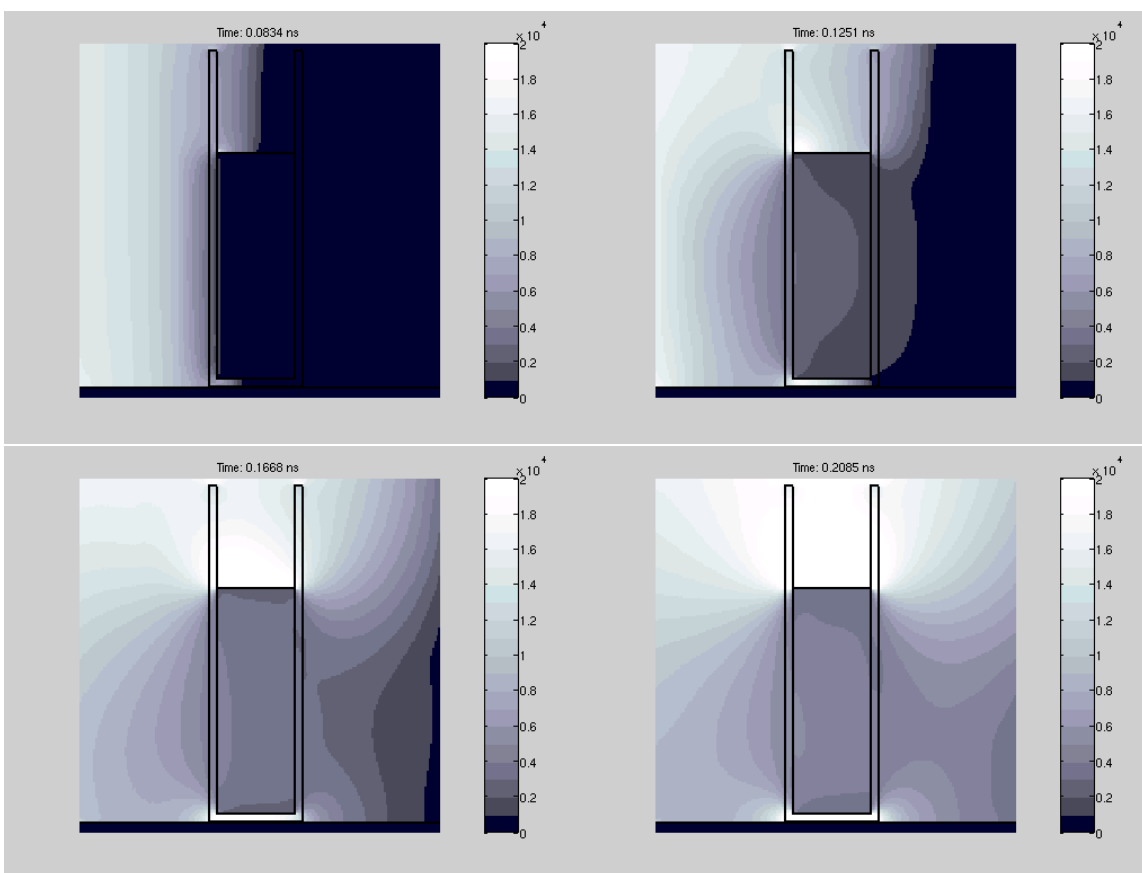


Figure 6. Penetration of an EM pulse into a blood-filled polystyrene cuvette. Contours represent the y -component of the electric field in steps of 1000 V/m .

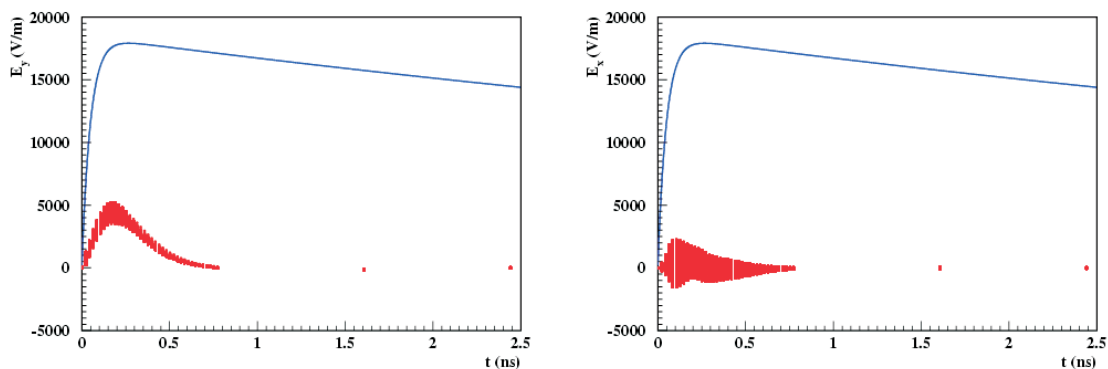


Figure 7. Comparison of components of the electric field in the blood-filled cuvette to shape of the incident pulse for a span of 2.5 ns . Distribution of the field values in a particular time is a measure of the inhomogeneity of the field across the sample.

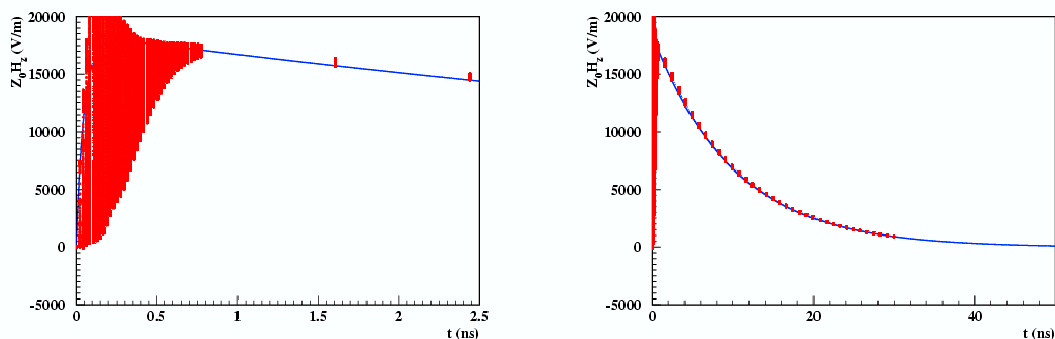


Figure 8. Magnetic field component multiplied by the impedance of free space, $Z_0 = 376.7 \Omega$. Left, field components (red vertical lines) are superimposed to the shape of the incident pulse for the first 2.5 ns. Right, calculated data for 50 ns. The distribution of the field values in a particular time is a result of inhomogeneity of the field across the sample.

- Penetration of the electric component in the direction of polarization (y) is defined by both rise time and pulse width. The pulse inside water is a superposition of a short pulse, induced by a fast rise time, and the longer incident pulse (Figure 9).
- The electric field perpendicular to the direction of polarization (x) is defined by rise time only (Figure 9).
- The magnetic field component is at first dominated by electrical induction, and, as the penetrated electric field components fall to zero, behaves as though no material were present, as in the case of blood.

Bacterial growth medium was simulated as water with a conductivity of 11.6 mS/m . The results agree with expectations based on the calculations on blood and water. The shape of the electric component in the direction of polarization is in essence similar to that for pure water. The width, however, is shortened by the low conductivity, as shown in top panel of Figure 10. The bottom panel shows the result of the calculation for cortical bone, the biomaterial least similar to water.

It became apparent in the course of this work that pulse penetration is a function of both rise time and pulse width. For a non-conductive material, both pulse features are important. For a conductive material, depending on conductivity, penetration is dominated by rise time. For blood, a material of considerable conductivity, incident pulse width is relatively unimportant. Left side of Figure 11 shows the penetration of a nanopulse inside a material as a function of conductivity. As conductivity increases amplitude and width of the penetrating pulse decrease; the pulse becomes a function of rise time only. In the right side of Figure 11, the conductivity of water was a constant 0.5 S/m while the pulse rise time varied from 780 ps to 100 ps .

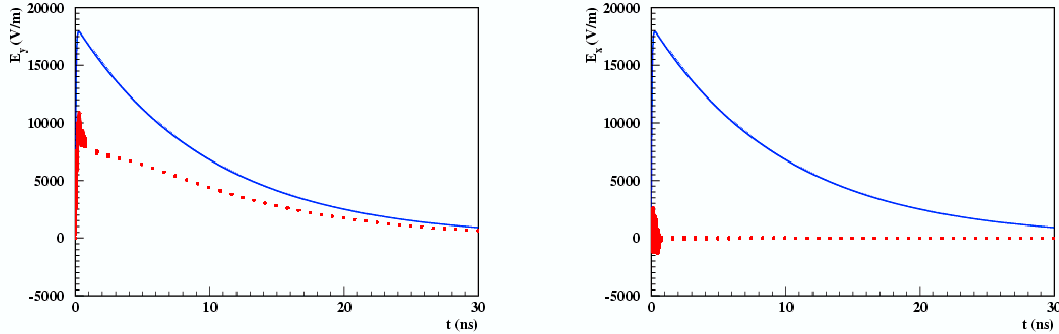


Figure 9. Components of the electric field inside water (red) plotted with incident pulse (blue) for the first 30 ns. The distribution of field components for a particular time point reflects the inhomogeneity of the field across the sample.

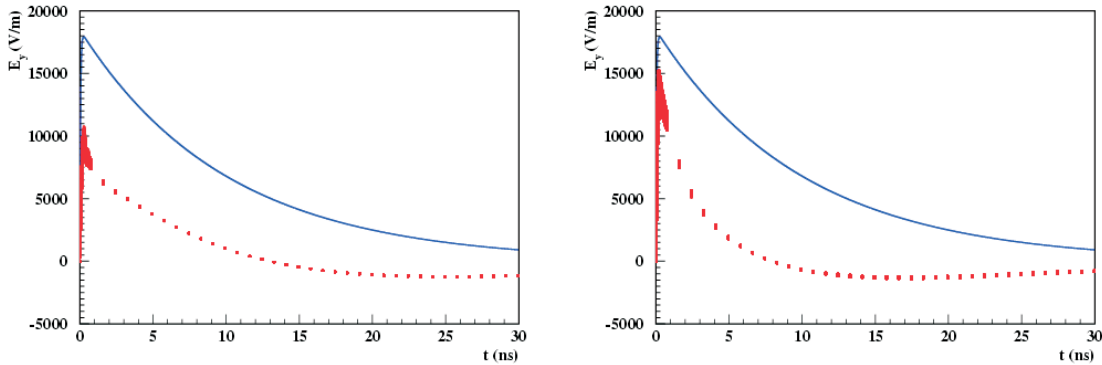


Figure 10. Electric field in the direction of polarization in bacterial growth medium (left) and in cortical bone (right), plotted with the shape of the incident pulse in the first 30 ns. The distribution of the field values for a particular time point measures inhomogeneity of the field across the sample.

FDTD also allows quick calculation of the pulse energy deposited in a biological material. Conversion of electromagnetic energy into mechanical or thermal energy is computed using [11]

$$P = \int_V \vec{J} \cdot \vec{E} dV, \quad (16)$$

where P is deposited energy in unit of time, and \vec{J} and \vec{E} are, respectively, current density and electric field inside the material. FDTD provides the values of \vec{E} and \vec{J} (from Equation 13) through the entire volume at any time. Numerical integration of Equation 16, used to determine the amount of energy deposited per pulse, is straightforward. The results show that this energy is small and does not influence the temperature of the exposed material for the pulse repetition rates of the order of few MHz or less.

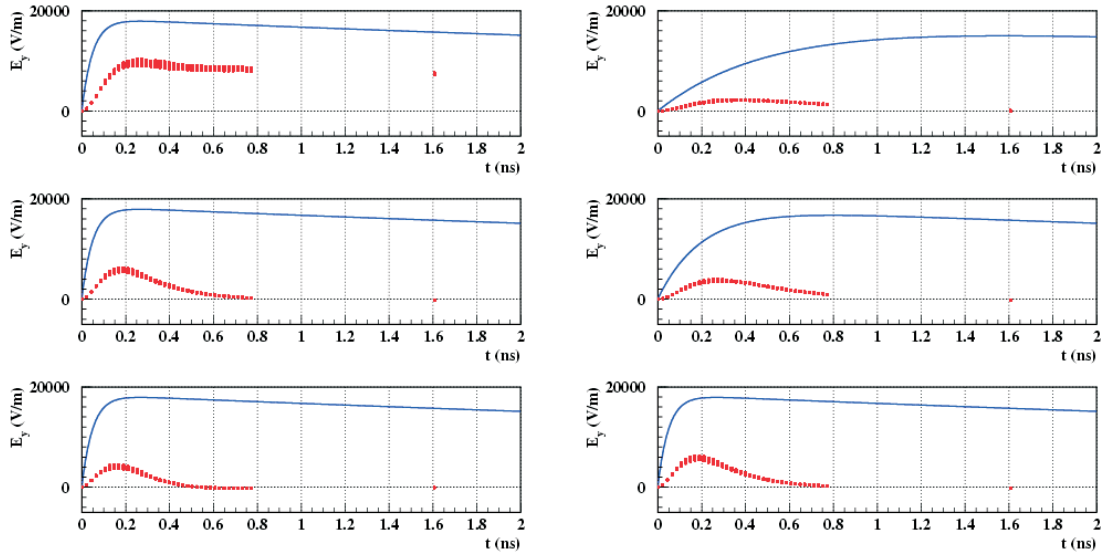


Figure 11. Left side: Electric field in the direction of polarization inside water with a conductivity of 0 S/m (top), 0.5 S/m (middle), and 1 S/m (bottom). The rise time of the incident pulse was 100 ps in each case. Right side: Electric field in the direction of polarization inside water of conductivity 0.5 S/m . The incident pulse rise time was 780 ps (top), 380 ps (middle), and 100 ps (bottom).

The average converted energy per pulse of the pulse described by Equation 1 was $\sim 0.003\text{ J/m}^3$ for blood and $\sim 0.0005\text{ J/m}^3$ for water. The resulting temperature increase, about $\sim 10^{-10}\text{ K}$ per pulse, is clearly negligible.

Finally, the power spectrum or spectral energy density must be modeled to understand the interaction of short EM pulses with biological material. The spectrum for the cases of blood and water, obtained by Fourier transformation of Equation 16, is shown in Figure 12.

4. Conclusion

We have presented a series of results of FDTD calculations on nanopulse (ultra-wideband) penetration of biological matter. Calculations included a detailed geometrical description of the material exposed to nanopulses, which is typically contained inside a cuvette or a Petri dish in an exposure chamber (*e.g.* GTEM cell), and a state-of-the-art description of the physical properties of the material. To ensure that the results would be sound, the length of a side of the Yee cell was set at $1/4\text{ mm}$, smaller than the value required by the cut-off frequency of 100 GHz , and the Cole-Cole parametrization of the dielectric properties of tissue in the frequency range $\leq 100\text{ GHz}$ was used to describe the exposed material. To minimize computation time, the Cole-Cole parametrization was reformulated in terms of the Debye parametrization with no loss of accuracy of description. In 2-dimensional FDTD, the decreased computation time enabled comparison of different materials on exposure to nanopulses. The results

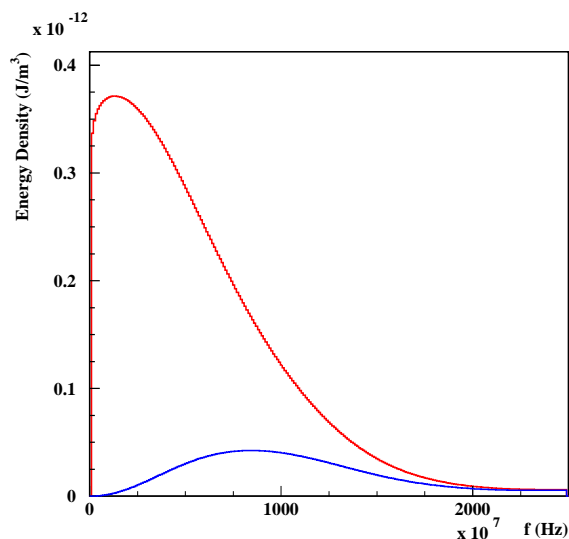


Figure 12. Spectral energy density for blood (upper red curve) and water (lower blue curve). The integral of a distribution over all frequencies is the total pulse energy.

can be summarized as follows:

a) The shape of a nanopulse inside a biomaterial is a function of both rise time and width of the incident pulse. The importance of the rise time increases and becomes dominant as the conductivity of the material increases.

b) Biological cells inside a conductive material are exposed to pulses defined by rise time only, which is often substantially shorter than the duration of the incident pulse. It is possible to define the pulse inside the material by the conductivity of the material and the rise time of the incident pulse.

c) The amount of energy deposited by the pulse is so small that no effect observed on exposure of a biological sample to nanopulses of ~ 20 kV/m amplitude will have a thermal origin.

Calculation of the electric field surrounding a biological cell is the first step in understanding any effect resulting from exposure to nanopulses. Fast and accurate numerical programs are necessary not only for such computation but also for optimization of future experiments. Results of the 2-dimensional FDTD calculations reported here have been compared in selected cases with the full 3-dimensional calculation. No significant difference in pulse propagation has been found thus far. Graphical results of the full 3-dimensional computation will be reported in a subsequent paper.

Acknowledgments

We thank Weizhong Dai, Shengjun Su, and other members of the research team for helpful discussions.

This material is based on research sponsored by the Air Force Research Laboratory,

under agreement number F49620-02-1-0136. The U.S. Government is authorized to reproduce and distribute reprints for Governmental purposes notwithstanding any copyright notation thereon. The views and conclusions contained herein are those of the authors and should not be interpreted as necessarily representing the official policies or endorsements, either expressed or implied, of the Air Force Research Laboratory or the U.S. Government.

References

- [1] Taylor J D ed. 1995 *Introduction to Ultra-Wideband Radar Systems* Boca Raton: CRC Press LLC.
- [2] Polk C and Postow E eds. 1995 *Handbook of Biological Effects of Electromagnetic Fields* Boca Raton: CRC Press LLC.
- [3] Sunkam R K, Hill J S, Selmic R R, and Haynie D T 2004 **Rev. Sci. Instrum.**, accepted for publication
- [4] Yee K S 1966 *IEEE Trans. Antennas Propagat.* **AP-14** 302
- [5] Sadiku M N O 1992 *Numerical Techniques in Electromagnetics* Boca Raton: CRC Press LLC.
- [6] Kunz K and Luebbers R 1993 *The Finite Difference Time Domain Method for Electromagnetics* Boca Raton: CRC Press LLC.
- [7] Sullivan, D M 2000 *Electromagnetic Simulation Using the FDTD Method* New York: Institute of Electrical and Electronics Engineers.
- [8] Taflov A and Hagness S C 2000 *Computational Electrodynamics: The Finite-Difference Time-Domain Method, 2nd ed.* Norwood: Artech House.
- [9] Bao J-Z 1997 *Rev. Sci. Instrum.* **68** 2221
- [10] Samn S and Mathur S 1999 *Preprint* AFRL-HE-BR-TR-1999-0291, McKesson HBOC BioServices Brooks AFB.
- [11] Jackson J D 1999 *Classical Electrodynamics* New York: John Willey & Sons Inc.
- [12] Luebbers R J, Hunsberger F, Kunz K S, Standler R B, and Schneider M 1990 *IEEE Trans. Electromagn. Compat.* **32** 222
- [13] Lubbers R J, Hunsberger F, and Kunz K S 1991 *IEEE Trans. Antennas Propagat.* **39** 29
- [14] Bui M D, Stuchly S S, and Costache G I 1991 *IEEE Trans. Microwave Theory Tech.* **39** 1165
- [15] Lubbers R J and Hunsberger F 1992 *IEEE Trans. Antennas Propagat.* **40** 1297
- [16] Gabriel C 1996 *Preprint* AL/OE-TR-1996-0037, Armstrong Laboratory Brooks AFB, <http://www.brooks.af.mil/AFRL/HED/hedr/reports/dielectric/home.html>
- [17] Gabriel S, Lau R W and Gabriel C 1996 *Phys. Med. Biol.* **41** 2251
- [18] Su S, Dai W, Haynie D, Nassar R and Simicevic N 2004 **XXX**, accepted for publication
- [19] Landau L D and Lifshitz 1960 *Electrodynamics of Continuous Media* Reading: Addison-Wesley Inc.
- [20] Schwartz J L and Mealing G A R 1985 *Phys. Med. Biol.* **30** 117
- [21] Hahn G M, Kernahan P, Martinez A, Pounds D and Prionas S 1980 *Annals of the New York Academy of Sciences* 327
- [22] Cook H 1952 *British Journal of Applied Physics* **3** 249
- [23] Pfutzner H 1984 *Medical and Biological Engineering and Computing* **22** 142
- [24] Burdette E C, Cain F L and Seals J 1980 *IEEE Trans. on Microwave Theory and Techniques* **4** 414
- [25] Alison J M and Sheppard R J 1993 *Phys. Med. Biol.* **38** 971
- [26] Schwan H P 1963 *Biophysik* **1** 198
- [27] Chang A T C and Wilheit T T 1979 *Radio Science* **14** 793
- [28] <http://caps.phys.latech.edu/~neven/pulsefield/>